

A Nonlinear Model for Collicular Spatial Interactions Underlying the Metrical Properties of Electrically Elicited Saccades

A. J. Van Opstal and J. A. M. Van Gisbergen

Department of Medical Physics and Biophysics, University of Nijmegen, Geert Grooteplein Noord 21, 6525 EZ Nijmegen, The Netherlands

Abstract. An earlier model for the collicular role in the generation of saccades (Van Gisbergen et al. 1987), based on ensemble coding and linear vector addition of movement contributions from independent movement cells, yields normometric saccades in all directions over a considerable range of amplitudes. The model, however, cannot account for two nonlinear phenomena which are known from collicular electrical stimulation experiments: 1) saccade amplitude has a roughly sigmoid dependence upon current strength and 2) two electrical stimuli applied simultaneously at different sites yield a response that resembles a weighted average of the individual responses. In the present paper we propose an intracollicular mechanism which, based on lateral spatial interactions in the deeper layers of the colliculus, results in nearby excitation and remote inhibition when current is applied. Both nonlinear phenomena can thus be explained. The possibility of excitatory and inhibitory collicular interactions is supported by recent evidence in the literature. The nonlinearity in the model, essential to explain the electrical stimulation findings, resides in the input-output characteristic of the deeper layer movement cells. The results, obtained by quantitative simulations with the model, are discussed together with possible alternative explanations.

1 Introduction

1.1 Early Models of the Superior Colliculus

The well-established fact that cells in the deeper layers of the Superior Colliculus (SC) possess quite extensive movement fields (Wurtz and Goldberg 1972; Sparks et al. 1976; Sparks and Mays 1980) implies that a large population of these so-called movement cells is active whenever a saccade is executed. It is known from single unit and electrical stimulation studies (Schiller and

Stryker 1972) that the motor colliculus is a topographically organized structure which embodies a so-called motor map (Robinson 1972). Sparks et al. (1976) and McIlwain (1976, 1982) postulated that every cell in the active population contributes to the total saccade by generating a small movement contribution whose size and direction depend on the cell's location in the collicular motor map. Vectorial summation of all these individual movement contributions in the system downstream then would yield the actual saccade vector. It is well established that, while activity in the rostral colliculus yields a small eye movement, a larger saccade results when the active population of collicular movement cells shifts more caudally (Robinson 1972; Sparks et al. 1976; McIlwain 1982). To explain this finding, McIlwain (1976, 1982) and Sparks et al. (1976) proposed that cells in the caudal part of the colliculus yield larger movement contributions than more rostral cells.

To account for the relation between the location of activity in a large population of collicular movement cells and the metrical properties (i.e. amplitude and direction) of the ensuing saccadic eye movement we have recently proposed a quantitative model of the monkey SC (Van Gisbergen et al. 1987; Van Opstal and Van Gisbergen 1989). As pictorially summarized in Fig. 1, the model incorporates the basic ideas about the role of ensemble coding in collicular function first expressed by McIlwain (1976, 1982) and Sparks et al. (1976). These notions were expressed mathematically and electrophysiological data from a small number of movement cells (Ottes et al. 1986), together with Robinson's (1972) electrical stimulation map were used to estimate the fixed parameters of the ensemble-coding model (Ottes et al. 1986; Van Gisbergen et al. 1987).

In this paper we explore the possible role of lateral interactions in the deeper layers of the superior colliculus in order to explain two findings from

collicular electrical stimulation experiments that cannot be understood from the simple ensemble-coding model: (1) saccade amplitude and electrical current strength are nonlinearly related (Sparks and Mays 1983); (2) the application of two simultaneous electrical stimuli at different collicular sites causes saccade averaging responses (Robinson 1972; Schiller and Sandell 1983; see below). Since the present model is an extension of the originally proposed ensemble-coding model, the latter will be briefly described first. For a full description of the model we refer to the original papers (Ottes et al. 1986; Van Gisbergen et al. 1987; Van Opstal and Van Gisbergen 1989).

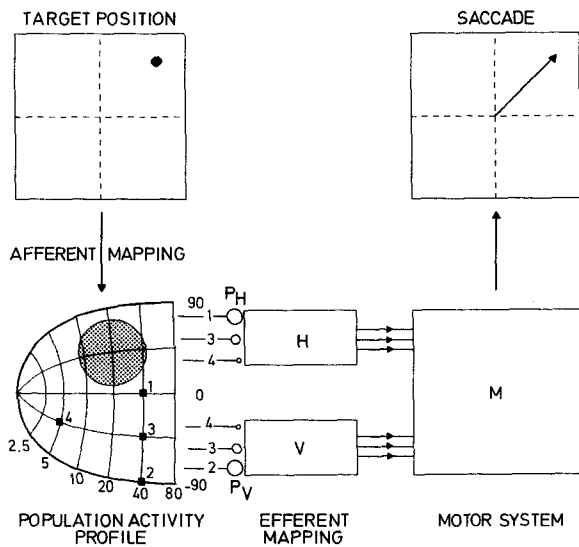


Fig. 1. Scheme summarizing the ensemble coding model of Van Gisbergen et al. (1987). The presentation of a visual stimulus at ($R_T = 20$, $\Phi_T = 45$ deg) gives rise to a Gaussian-shaped population activity profile at the corresponding location in the deeper layers of the colliculus (afferent mapping stage). Each movement cell is connected to the horizontal (H) and vertical (V) premotor systems through connection strengths P_H and P_V , respectively. As symbolized by the size of the synaptic connections with H and V , caudal cells (e.g. 1, 2, and 3) have stronger efferent connections than more rostral cells (4). Equal direction (-90 , -45 , 0 , 45 , 90) and equal magnitude (2.5, 5, 10, 20, 40, 80) contours of the movement potential of each movement cell have been depicted superimposed on the colliculus. Depending on the location relative to these equal direction contours, the cells are connected to the horizontal (1), the vertical (2) or both subsystems (3 and 4). The equal magnitude contours specify the strength of these synaptic contacts. The motor system, M , represents the mechanical geometry of the six eye muscles. For simplicity it is assumed, in the model, that the eye muscles are orthogonally organized along the three cardinal directions (horizontal, vertical and torsion). Effectively there is no net torsion in the model for visually-guided saccades (Listing's law), since none of the movement cells is endowed with a torsional movement contribution. All contributions of the recruited cells are summed at the motor stage and finally result in an eye movement that is directed to the position of the stimulus

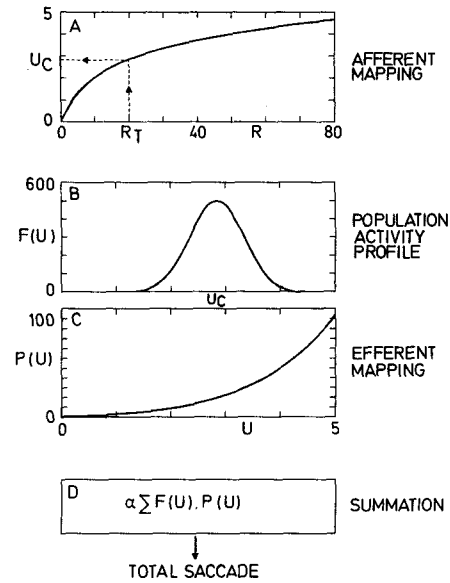


Fig. 2A-D. One-dimensional representation of the ensemble-coding model of Van Gisbergen et al. (1987). **A** The afferent mapping function determines the collicular locus, u_c [mm from the foveal representation], corresponding to target eccentricity, R_T [deg], by the logarithmic function: $u_c = B_u \cdot \ln[1 + R_T/A]$, where $A = 3.0$ deg and $B_u = 1.4$ mm. **B** The active population, $F(u)$, is centered around u_c and is described by a Gaussian function [$\sigma = 0.5$ mm; $F_{max} = 500$ spikes/s]. **C** The efferent mapping function, $P(u)$, describes the connection strength of each cell with the premotor system downstream by the exponential function: $P(u) = A \cdot [\exp(u/B_u) - 1]$. Note, that $P(u)$ is the mathematical inverse of the afferent mapping function. **D** The actual contribution of a recruited cell, $M(u)$, is given by the product, $\alpha \cdot F(u) \cdot P(u)$ (see text). The amplitude of the saccade is then determined by linear summation of all cell movement contributions

Basically, the ensemble-coding model consists of three serially-arranged stages denoted as the afferent mapping mechanism, the population activity profile and the efferent mapping mechanism, respectively (Figs. 1 and 2). The afferent mapping mechanism describes the collicular locus of the center of movement-cell activity for each target location in visual space by a two-dimensional complex-logarithmic function (Fig. 2A). It was found by Ottes et al. (1986) that the spatial extent of the population of recruited movement cells, whose center location is determined by the afferent mapping function, can be approximated by a Gaussian function with an estimated standard deviation (σ) of about 0.5 mm (see Fig. 2B). In the ensemble-coding model the activity profile is translation invariant except for truncation at the collicular borders.

The efferent mapping mechanism of the model (Fig. 2C) specifies how each active cell contributes to the total saccade. The contribution of a particular

movement cell in the model is determined by its firing rate and the nature and the strength of its efferent connections which specify its potential to create movement. To express this potential mathematically, Van Gisbergen et al. (1987) assigned a so-called movement-potential vector to each movement cell (see legend Fig. 2). Although this is certainly a simplification, (see e.g. Ferman et al. 1987) it was assumed that Listing's law (Carpenter 1977) is valid for visually-elicited saccades starting in the primary position. Accordingly, the movement-potential vector is defined in a two-dimensional (horizontal-vertical) motor frame.

Finally, as proposed by Sparks et al. (1976) and McIlwain (1976, 1982), all individual movement contributions are summed vectorially in order to determine the metrics of the saccade (Fig. 2D).

1.2 Evaluation of the Ensemble-Coding Model

It appeared that the ensemble-coding model, despite its extreme simplicity, can produce normometric saccades in all directions over a considerable amplitude range and can simulate both Robinson's (1972) electrical stimulation map of the monkey colliculus and the shape of movement fields of deeper-layer collicular cells (Ottes et al. 1986). In the simulations of Robinson's electrical-stimulation data it was assumed that the suprathreshold electrical stimulus in his experiments always created the same population-activity profile. However, it is known that lowering the electrical stimulus strength, which affects the size of the active population (Stoney et al. 1968; Alexander and Delong 1985; see also below), causes saccade amplitude to shrink (Sparks and Mays 1983). The existing ensemble-coding model fails to account for this relation between current strength and saccade amplitude and, in particular, cannot explain why saccade amplitude does not increase further beyond a certain current strength (Van Opstal and Van Gisbergen 1989).

There is an additional consistent finding in electrical stimulation experiments which cannot be understood from the existing ensemble-coding model: when *two* electrical stimuli are applied simultaneously at different sites in the deeper layers (Robinson 1972) the resulting saccade resembles a weighted average of the two individual stimulation effects. The weighting factors depend upon the relative current strengths at the two sites. This effect cannot be explained by the existing ensemble-coding model which always predicts that the saccade is the linear vector sum of the two stimulus contributions. In this context it is useful to note that since the nonlinear afferent and efferent mapping are the inverse of one another, the overall behaviour of the ensemble coding model, except for border truncation effects, is linear. Therefore it is

understandable that it can explain neither the averaging phenomenon nor the sigmoid relation between saccade amplitude and electrical current strength which both require an overall nonlinear model.

1.3 Can Averaging be due to Collicular Lateral Interactions?

We first wish to consider briefly two logical possibilities for including a nonlinearity in the model to explain the double stimulation experiments and the saturation of saccade amplitude for high stimulus intensities. First, the nonlinearity may be an intracollicular mechanism: in the case of electrical double stimulation in the deeper layers, the population activity profile resulting from simultaneous stimulation at two locations is almost certainly not simply the linear sum of the individual stimulation effects. Second, the nonlinearity may be located downstream of the colliculus. For example, it might be supposed that the movement contribution of a given cell is not solely determined by its own firing rate, but is scaled down dependent upon the total movement cell activity of the colliculus. This possibility will be discussed below (see Discussion).

This paper explores how intracollicular interactions may be responsible for the nonlinear effects described in electrical stimulation studies. Before the revised model is presented we review some recent experimental work which supports the notion of intracollicular spatial interactions.

1.4 Evidence for Lateral Interactions in the Superior Colliculus

It was found by McIlwain (1982) that intracollicular electrical stimulation in the intermediate gray layer of the cat induces spike activity in cells up to 1 mm from the stimulation site. Since the latency had a mean value of about 1.5 ms it was argued that the resulting activity could not merely be due to current spread or to antidromic activation of the recorded cell. McIlwain suggested that lateral excitatory connections within the collicular layer over a considerable distance are probably responsible.

Quite recently Douglas and Vetter (1986) have claimed the existence of lateral inhibitory interactions in the cat's colliculus. After application of glutamate, used to increase the collicular background firing rate, subsequent electrical stimulation at a particular site produced a noticeable decrease of the background firing rate throughout both colliculi after latencies between 3–10 ms. Following section of the intertectal commissure the contralateral inhibition disappeared suggesting that the commissure carries an inhibitory signal between the two colliculi. Douglas and Vetter

proposed that the lateral inhibition is mediated through a layer of inhibitory collicular interneurons.

Infante and Leiva (1986) recorded simultaneous single-unit activity in both colliculi of the cat while the animal was making saccades in various directions. They found that the movement-related spike activity in both colliculi seems to be reciprocally related: an increase of the activity in one colliculus is accompanied by a decrease of activity in the other colliculus and vice versa.

The notion of intercollicular inhibition also seems to be supported by a recent study of Schiller et al. (1987). Reversible inactivation of one colliculus by muscimol or, alternatively, by complete ablation of one colliculus causes onset latencies of ipsilateral saccades to decrease when compared to the situation where both colliculi are still intact. These experiments suggest a disinhibition of the remaining colliculus after inactivation of the other colliculus.

Finally, the so-called remote stimulus effect in collicular neurons (Rizzolatti et al. 1973, 1974, in cat; Wurtz et al., 1980, in monkey) also indicates the possibility of lateral inhibitory interactions. Wurtz and co-workers found that a remote stimulus, which by itself does not cause a response, may severely reduce the excitatory effect of a stimulus in the central activating area of the receptive field. They found that the spatial extent of the inhibition may be beyond 50 deg and may cross the vertical meridian. Unfortunately it is not known whether these effects in superficial layer cells can also be observed in deeper layer neurons.

1.5 Outline of the Nonlinear Lateral-Interaction Model

In this paper we extend the existing ensemble-coding model by allowing excitatory and inhibitory spatial interactions: in line with the work cited above (McIlwain 1982; Douglas and Vetter 1986; Infante and Leiva 1986), the population-activity profile is no longer exclusively excitatory. We propose instead that, due to lateral interactions within the colliculus, an electrical point stimulus gives rise to a population activity profile characterized by local excitation and remote inhibition. How such a population activity can be mediated by a neural network is a separate problem which will not be dealt with in the present paper. The essential nonlinearity, required if the model is to explain the nonlinear averaging phenomenon (see above), is proposed to reside in the input-output characteristic of the movement cells. A schematic outline of the model is presented in Fig. 3. As will be shown below (see Results) the new model can simulate that saccade amplitude is nonlinearly related to electrical stimulation intensity. In addition, when two

stimuli are applied simultaneously, the saccade predicted by the new model appears to be a weighted average of the two stimulation effects. In the next section a detailed mathematical description of the model will be presented. Part of these results have been published elsewhere in a preliminary form (Van Opstal and Van Gisbergen 1987).

2 Mathematical Description of the New Model

The original ensemble-coding model (see Figs. 1 and 2) does not specify precisely *how* the population-activity profile comes about. The present nonlinear model, however, has three additional stages which specify how lateral interactions result, finally, in the population activity profile (see below). A schematic outline of the new model, in the format of Fig. 2, is presented in Fig. 3. In the model we propose that electrical stimulation by a microelectrode leads to two opposite effects on nearby collicular movement cells which can be characterized by local excitation and remote inhibition. For ease of description, we will describe these two effects separately, leaving aside the precise mechanisms that may underly them. In what follows, the colliculus has been assigned a Cartesian coordinate grid $[(u, v; \text{in mm})]$ see Ottes et al. (1986) Van Gisbergen et al. (1987) for more details]. The three new features of the model: the excitation function, the lateral transmission function and the nonlinear input-output characteristic of the model neurons will now be briefly described.

2.1 Excitation Function

When a stimulating electrode applies current at collicular coordinates (u_c, v_c) , it is assumed that the excitatory effect, $E(u, v)$, decays with distance from the electrode tip according to a Gaussian function (see Fig. 3A):

$$E(u, v) = E_{\max} \cdot \exp \left[-\frac{(u - u_c)^2 + (v - v_c)^2}{2\sigma_a^2} \right]. \quad (1)$$

In this equation E_{\max} [mV] is the maximal excitatory effect of the stimulus and σ_a [mm] is a measure for the spatial extent of the resulting excitation which, in the model, is directly related to current strength. We have assumed, however, that $E(u, v)$ is broader than expected from the effects of physical current spread alone and includes the intracollicular spread of excitation found by McIlwain (1982). The relation between σ_a and current strength, I , (shown in Fig. 4) is derived from equations which are based on experimental data from Stoney et al. (1968) and Alexander and Delong (1985). In this paper it is assumed that I and σ_a are related through $\sigma_a = 0.5(I/40)^{1/2}$ mm (I in μA). A justification for this choice is given in Appendix I.

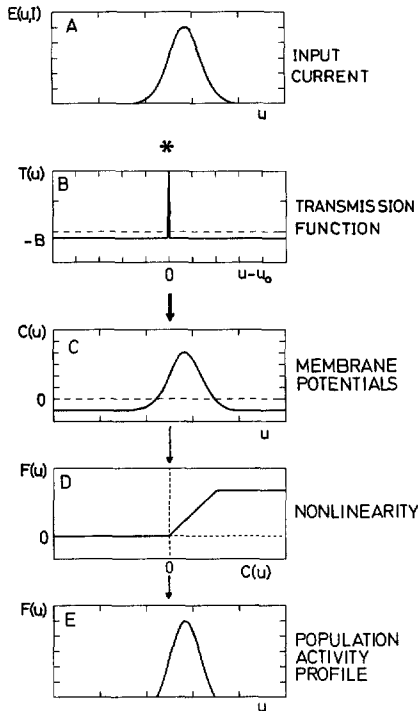


Fig. 3A-E. One-dimensional scheme of the various steps from electrical stimulation to population-activity profile in the new model. **A** Application of current, I , to the deeper layers excites cells, surrounding the electrode tip, according to a Gaussian function, $E(u, I)$. The width of the excitation profile, σ_a , depends on current strength according to the relation shown in Fig. 4. **B** Each excited cell exerts inhibition on all other cells, except on itself. The lateral transmission function, $T(u)$, has a constant strength, B , throughout both colliculi. **C** The combined effect of excitation (**A**) and lateral inhibition (**B**), found by convolution, leads to a distribution of cell membrane-potentials, $C(u)$, characterized by local excitation and remote inhibition. **D** The firing rate, F_i , of a particular cell, i , depends nonlinearly on its membrane potential, C_i : for negative potentials the cell will not be recruited ($F_i=0$) whereas for positive C_i firing rate increases linearly up to the maximum activity of 500 spikes/s. It is assumed that movement cells have no resting activity and that the recruitment threshold is 0 mV. **E** Applying the nonlinear input-output characteristic of each movement cell (**D**) on the total distribution of cell membrane-potentials (**C**) finally yields the population activity profile, $F(u)$

2.2 Lateral Transmission Function

It is assumed that excitation of a given cell in the deeper layers at (u_0, v_0) , causes a change, $T(u, v)$, in the membrane potential of a large population of adjacent neurons, which can be described by a global inhibitory field of constant strength which surrounds the neuron under study (see Fig. 3B). This can be formulated mathematically by:

$$T(u, v) = T_{\max} \cdot \delta(u - u_0, v - v_0) - B, \quad (2)$$

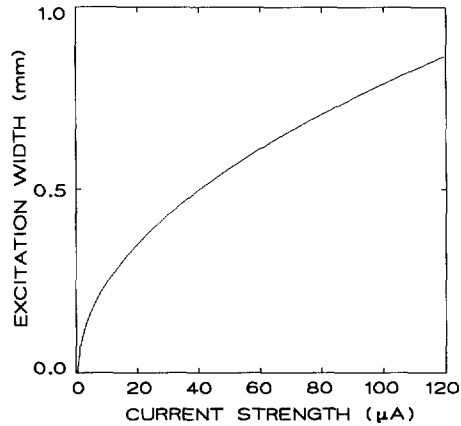


Fig. 4. Relation between current strength (I) and width of the excitatory profile (σ_a) used in the simulations. The relation [$\sigma_a = 0.5 \cdot (I/40)^{1/2}$ mm] is derived from equations proposed by Stoney et al. (1968). See also Appendix I

where T_{\max} and B [dimensionless and mm^{-2} , respectively, see Appendix II] are constants and $\delta(u, v)$ is the Dirac delta-function. Equation (2), which can be interpreted as the spatial impulse response of the collicular network, thus states that each excited neuron exerts an inhibitory influence on every other collicular movement cell (extending to *both* colliculi) of constant strength, except on itself.

The total change, $C(u, v)$, in a given cell's membrane potential, after electrical stimulation is given by the convolution of the excitation function imposed by the electrical stimulus (1) and the lateral transmission function (2):

$$C(u, v) = \iint dpdq T(u-p, v-q) E(p, q), \quad (3)$$

where p and q are integration variables. Assuming linear addition of effects prior to the stage of spike generation, it can be shown (see Appendix II) that the combined effect of (1) and (2) leads to a Gaussian excitatory profile surrounded by a field of constant inhibition (Fig. 3C). The strength of the resulting inhibition will depend on the width of the excitation function, σ_a , and hence on the electrical current strength (for details see Appendix II).

2.3 Nonlinear Input-Output Characteristic

It is assumed that deeper layer movement cells are not spontaneously active (see e.g. Sparks and Mays 1980). The firing rate of a cell at location (u, v) , denoted by $F(u, v)$, is proposed to depend *nonlinearly* on the membrane potential $C(u, v)$. When $C(u, v)$ (3) is negative, the cell is under inhibition and will not fire, whereas an excitatory membrane potential leads to a linear increase in the cell's firing rate (slope β ,

[spikes/mV]) until the cell's maximum firing rate, F_{\max} (set at 500 spikes/s), is reached (see Fig. 3D). Note, that it is assumed that the threshold, θ , for spike generation equals 0 mV.

Once the collicular population activity, $F(u, v)$, is computed, (Fig. 3E) the computation of the movement contributions of individual cells to the total saccade is straightforward. From here on the model is exactly the same as the original ensemble coding model (Figs. 1 and 2; Van Gisbergen et al. 1987; Van Opstal and Van Gisbergen 1989). Thus, each cell's vectorial movement contribution $\mathbf{M}(u, v)$, is determined by its location (u, v) in the motor layer (which determines the synaptic strengths $\mathbf{P}(u, v)$ with the horizontal and vertical subsystems downstream) and its firing rate, $F(u, v)$:

$$\mathbf{M}(u, v) = \alpha \cdot F(u, v) \cdot \mathbf{P}(u, v), \quad (4)$$

where α [(spikes/s) $^{-1}$] is a fixed proportionality constant which is identical for all cells (see Van Gisbergen et al. 1987, for more details).

Finally, vectorial summation of all cell contributions (Fig. 2D), results in the metrics of the saccadic eye movement. It should be noted, that since the inversely related logarithmic afferent and exponential efferent mapping functions cancel each other completely, the nonlinear input-output characteristic of the model neurons (Fig. 3D) solely determines the overall nonlinearity of the model: since the movement cells exhibit no resting activity (see above), inhibition can only exert its influence on a cell's movement contribution when the cell is excited, by decreasing its activity (see Results, e.g. Fig. 6).

Note that in the model a cell's movement contribution is still uniquely determined by its firing rate and its efferent connections (Van Gisbergen et al. 1987; Van Opstal and Van Gisbergen 1989).

3 Simulations

The model consists of a square-lattice array of collicular neurons arranged in rows parallel with the horizontal meridian representation (u -axis) and in columns along the perpendicular collicular dimension (v -axis; see also Ottes et al. 1986; Van Gisbergen et al. 1987). Both colliculi are contained in one matrix of 64×64 neurons. Simulations were run on a PDP 11/44 computer.

3.1 Tuning the Model

In order to generate saccades with the correct metrics, it is necessary to tune the various proportionality constants in the model (E_{\max} , α , β , and F_{\max}) for given T_{\max} and B values of the lateral inhibition function (2). Without loss of generality (see Appendix II), T_{\max} and β were first set to 1.0 and 10 (spikes/s)/mV, respectively.

In this case B expresses the relative strength of inhibition. Since it is proposed that all the neurons have identical input-output properties (see above) and are distributed homogeneously in the colliculus, the proportionality constants only need to be determined for one particular site. Like in the earlier paper (see Van Gisbergen et al. 1987) the model parameters were found by stimulating with an intensity corresponding to $\sigma_a = 0.5$ mm (i.e. $I = 40 \mu\text{A}$, see Fig. 4 and Appendix II) at the collicular representation of the external world point with eccentricity $R = 20$ deg along the horizontal meridian to the right ($\Phi = 0$ deg) [i.e. $(u, v) = (2.85, 0)$ mm]. The resulting activity profile (after applying the nonlinear input-output characteristic of the model neurons) was then scaled in such a way that the most active cell reached the maximal activity of exactly $F_{\max} = 500$ spikes/s. In this way E_{\max} and F_{\max} were set simultaneously. Finally, the value of parameter α (4), needed to obtain a saccade amplitude of exactly 20.0 deg, was determined. Once these parameters were found, they were no longer subject to change in further simulations (see Results).

3.2 The Lateral Transmission Function

In order to find a suitable value for the relative inhibition strength, B , of the lateral transmission function (2), B was changed systematically in 0.0002 increments. The following two criteria were imposed: (1) changing the width, σ_a , of the excitation profile, (1) from 0.2 to 0.5 mm [corresponding, in the model, with current intensities between 6 and 40 μA , see Fig. 4 and Appendix II] had to result in at least a doubling of saccade amplitude and (2) increasing this width from 0.5 to 0.8 mm [current strengths between 40 and about 100 μA] should not result in a change of saccade amplitude of more than 10%. These criteria were set so that the model could qualitatively simulate the sigmoid relation between current strength and saccade amplitude (Sparks and Mays 1983; see also Fig. 5). Table 1 summarizes the values of the model parameters that have been used throughout this paper.

3.3 Electrical Double Stimulation

A straightforward procedure can be applied when electrical double stimulation at sites A and B is simulated. The two resulting excitatory profiles $E_A(u, v)$ and $E_B(u, v)$ are treated simultaneously in the procedures sketched above. The different current strengths at the two electrodes directly determine the corresponding excitatory profile widths, σ_{aA} and σ_{aB} , respectively (1). The effect of both stimuli on the membrane potential of each individual movement cell is then found by linear summation of the individual excitatory and inhibitory stimulation effects. Thus, the

Table 1. Parameter values of the nonlinear lateral interaction model used in the simulations in this paper. Parameters have been put together in separate groups, corresponding to the various stages in the model. The right-hand column refers to sections in this paper or to related papers where these parameters have been discussed. The value of $\alpha(4)$ is higher than in the Van Gisbergen et al. (1987) paper because in the present paper a smaller matrix has been used to describe the motor colliculus

Stage	Parameter	Value	Explanation
Afferent mapping	B_u	1.4 mm	Ottes et al. (1986)
	B_v	1.8 mm/rad	Ottes et al. (1986)
	A	3.0 deg	Ottes et al. (1986)
Activity profile	T_{\max}	1.0	Fig. 3B; Appendix II
	B	0.0032 mm^{-2}	Fig. 3B; Appendix II
	E_{\max}	50 mV	Fig. 3A; Appendix I
	k	$0 \mu\text{A}$	Fig. 4; Appendix I
	m	$40 \mu\text{A}/\text{mm}^2$	Fig. 4; Appendix I
Nonlinearity	β	10 (spikes/s)/mV	Fig. 3D
	F_{\max}	500 spikes/s	Fig. 3D
	θ	0 mV	
Efferent mapping	α	1.7×10^{-4} (spikes/s) $^{-1}$	Van Gisbergen et al. (1987)

total membrane potential of a given neuron at (u, v) will be $C(u, v) = C_A(u, v) + C_B(u, v)$. The firing rate of a cell at (u, v) , $F_{AB}(u, v)$, is then determined applying the nonlinear input-output characteristic of the neuron (Fig. 3D). In general, because of this nonlinearity, $F_{AB}(u, v)$ will not equal the linear sum of $F_A(u, v)$ and $F_B(u, v)$. It will be shown (see Results), that the metrics of saccades generated by the model, resemble a weighted average of the individual effects from each electrode.

4 Results

4.1 Relation Between Saccade Amplitude and Current Strength

Figure 5 shows the final result of the systematic search for a value of the relative strength of inhibition B that meets the imposed constraints (circles; see Simulations). It is clear from this figure that above a current strength of about $50 \mu\text{A}$ saccade amplitude does not increase further. Compared with the “best saccade” (filled dot) of this collicular locus (i.e. the saccade that is accompanied with the most vigorous discharge of the movement cells nearby the electrode tip) there appears a slight overshoot (less than 10%) in the range $40\text{--}90 \mu\text{A}$. It can also be observed that saccade amplitude starts to decrease again for extreme stimulus intensities ($>100 \mu\text{A}$, see Discussion). Saccade direction (not shown) appears to be independent from current strength in all simulations.

These results make clear that the model can, at least qualitatively, simulate the observed behaviour of saccade amplitude as a function of current strength by

assuming a relatively weak inhibition ($B=0.0032$) between cells. In Fig. 5 it is also shown how the model behaves when there is no inhibition ($B=0$, rectangles). In this case, which simulates in fact the original ensemble coding model of Van Gisbergen et al. (1987),

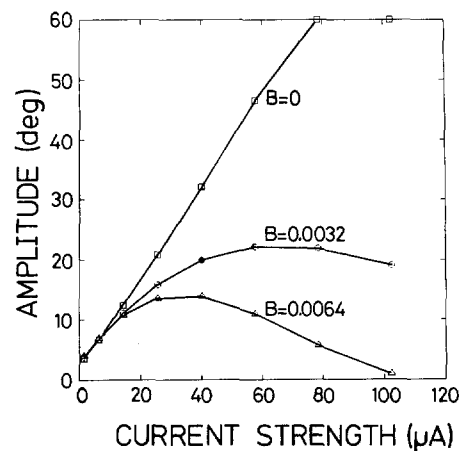


Fig. 5. Model simulations of saccade amplitude as a function of current strength for an inhibition strength of $B=0.0032 \text{ mm}^{-2}$ (open circles). The model was tuned such that a stimulus current of $40 \mu\text{A}$ at collicular coordinates ($u=2.85, v=0 \text{ mm}$), yielded a saccade size of exactly 20 deg (filled dot; see Simulations section). Saccade amplitude increases roughly linearly with current strength for low stimulus intensities but shows saturation beyond $50 \mu\text{A}$. Squares indicate the model's response when $B=0$ (no inhibition). Note that the saturation of saccade amplitude is absent (amplitude reached at $I=120 \mu\text{A}$ is 82.5 deg). Triangles show how the model behaves when the inhibition strength is doubled ($B=0.0064 \text{ mm}^{-2}$). Saccade amplitude decreases sharply for current strengths above $40 \mu\text{A}$.

saccade amplitude does not show saturation at all for the current strengths tested. Doubling the inhibitory strength ($B=0.0064$, triangles) leads to a reduction of saccade amplitude, already at moderate stimulus intensities. It is found that a 10% change of the value of parameter B has only a slight effect on the shape of the $R(I)$ -curve. Therefore, the overall behaviour of the model is not very sensitive to small changes in the relative inhibition strength B . In the results that follow, simulations are presented with the fixed set of parameters given in Table 1.

4.2 Response to Electrical Double Stimulation

In this simulation (Fig. 6) it is assumed that the stimulating electrodes are positioned at locations $(u, v)_A$ and $(u, v)_B$, corresponding to $(R, \Phi)=(10,0)$ and $(30,0)$, respectively (ΔR -experiment). Figure 6A shows three typical examples of the model's response to double stimulation when the current strengths at sites A and B were $[40, 25]$, $[40, 40]$, and $[25, 40]$ μA (nos. 1, 2, and 3, respectively; open circles in Fig. 6A). Filled circles correspond to the individual stimulation effects of electrodes A and B when a current of $40 \mu\text{A}$ is applied. Clearly, in the double stimulation situation the saccade always ends in between A and B . As the strength of stimulus B increases, relative to stimulus A , the metrics of the saccade corresponds more closely to the effect of stimulating site B alone (see also Fig. 8A).

In Fig. 6B the imposed activity profile, seen from above, is shown in the form of a contour plot for the case where A and B both equal $40 \mu\text{A}$. Figure 6C shows the population activity profile [shown in cross-section along the horizontal meridian representation ($v=0$)] for the case when only one stimulus at site $(u, v)_A$ or $(u, v)_B$ is present ($I=40 \mu\text{A}$). The double-stimulation situation (indicated as $A+B$) is also presented. From this figure it is especially clear how the spatial interactions in the model, in combination with the input-output nonlinearity of the movement cells, can cause averaging. Notice that, due to the movement cell nonlinearity (Fig. 3D), superposition does not hold. Accordingly, the firing-rate profile for the double-stimulation condition ($A+B$) is not simply the sum of profiles A and B but considerably less. The reason for this nonlinear phenomenon, in the model, is that the inhibition created, e.g. by stimulus A at site $(u, v)_B$, is only expressed in the firing rate of local cells if these neurons receive excitatory input, e.g. from stimulus B .

Notice furthermore that although the effects of a second stimulus at A or B are symmetrical in the collicular map (Fig. 6B and C), these effects are not symmetrical anymore at the level of the motor output (Fig. 6A), due to the nonlinear efferent mapping stage (Fig. 2D).

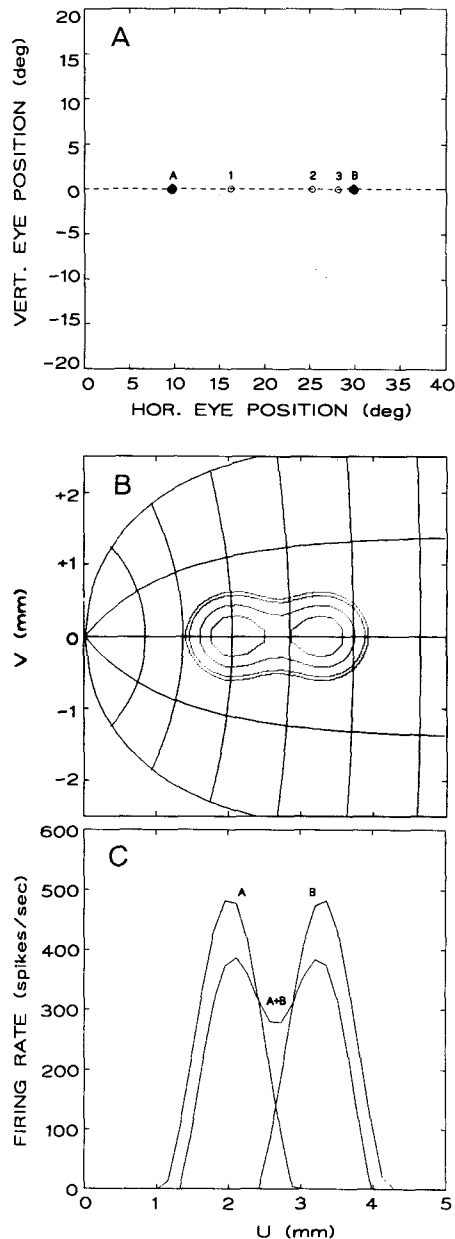


Fig. 6A–C. Simulations of ΔR electrical double stimulation experiment. Collicular coordinates $(u, v)_A$ and $(u, v)_B$ of sites A and B correspond with $(R, \Phi)=(10,0)$ and $(30,0)$, respectively. **A** Saccade endpoints for three double stimulation conditions (open symbols). Data point 1: $I_A=40 \mu\text{A}$, $I_B=25 \mu\text{A}$. Data point 2: $I_A=40 \mu\text{A}$, $I_B=40 \mu\text{A}$. Data point 3: $I_A=25 \mu\text{A}$, $I_B=40 \mu\text{A}$. In all three cases the saccade is directed in between the two single-stimulation endpoints A and B . **B** Activity profile in the motor colliculus giving rise to data point 2 (**A**) seen from above. Contours denote equi-activity lines corresponding with 65, 100, 200, and 300 spikes/s going from outside to inside. Superimposed on the motor colliculus is the movement potential of each movement cell (see also Fig. 1). **C** Cross section through **B** along the horizontal meridian representation ($v=0$). Clearly, the activity profile at locations u_A and u_B has decreased significantly with respect to the single stimulation effects (superimposed), due to the summed inhibitory effect of the recruited neurons

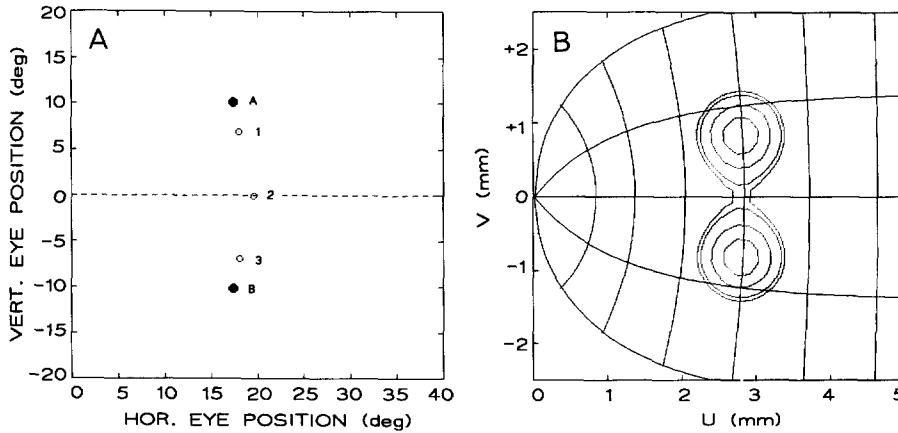


Fig. 7A and B. Simulation of $\Delta\Phi$ electrical double stimulation experiment at collicular coordinates $(u, v)_A$ and $(u, v)_B$ corresponding with $(R, \Phi) = (20, 30)$ and $(20, -30)$, respectively. **A** Saccade endpoints (open symbols) under the same conditions as in Fig. 6A. **B** Activity profile in the motor colliculus for condition nr. 2 ($I_A = I_B = 40 \mu\text{A}$). Same format as in Fig. 6B. Maximal activity has decreased to 360 spikes/s in this situation (see text for more details)

In Fig. 7 a typical result is shown for the case where the stimulation electrodes A and B are situated at the representations of $\Phi = 30$ deg and $\Phi = -30$ deg, respectively ($\Delta\Phi$ -experiment; eccentricity: $R = 20$ deg). The same three cases as shown in Fig. 6A are presented in Fig. 7A. Again it is clear that the resulting double-stimulation saccades are not the linear vector sums of A and B (filled circles), but resemble weighted averages (see also Fig. 8B). Figure 7B shows the activity profile (as seen from above) for stimulus pattern nr. 2 ($I_A = I_B = 40 \mu\text{A}$). Note that the collicular distance between $(u, v)_A$ and $(u, v)_B$ is larger in this $\Delta\Phi$ -experiment than in the ΔR -experiment of Fig. 6B so that there is less overlap between the two activation profiles. Because in the $\Delta\Phi$ -experiment the total population of recruited cells is larger, the strength of the reciprocal inhibition is also larger. Consequently, maximal activity at $(u, v)_A$ and $(u, v)_B$ has dropped even further to 360 spikes/s, compared with the single stimulus condition (500 spikes/s).

Figure 8A, B summarizes the dependence of saccade metrics on the relative strengths of the two stimuli. In Fig. 8A (ΔR -experiment, same stimulus locations as in Fig. 6) three conditions are shown which correspond to three different, but constant, current strengths of stimulus A (15, 25, and $40 \mu\text{A}$, respectively). Saccade amplitude is plotted as a function of the current strength of stimulus B . Note that saccade amplitude

increases roughly similarly under the three conditions as a function of the current strength of stimulus B .

Likewise, Fig. 8B shows the same situation as Fig. 8A for the $\Delta\Phi$ -experiment. It appears (not shown) that in this experiment saccade amplitude is roughly constant for the high intensity condition ($40 \mu\text{A}$) but

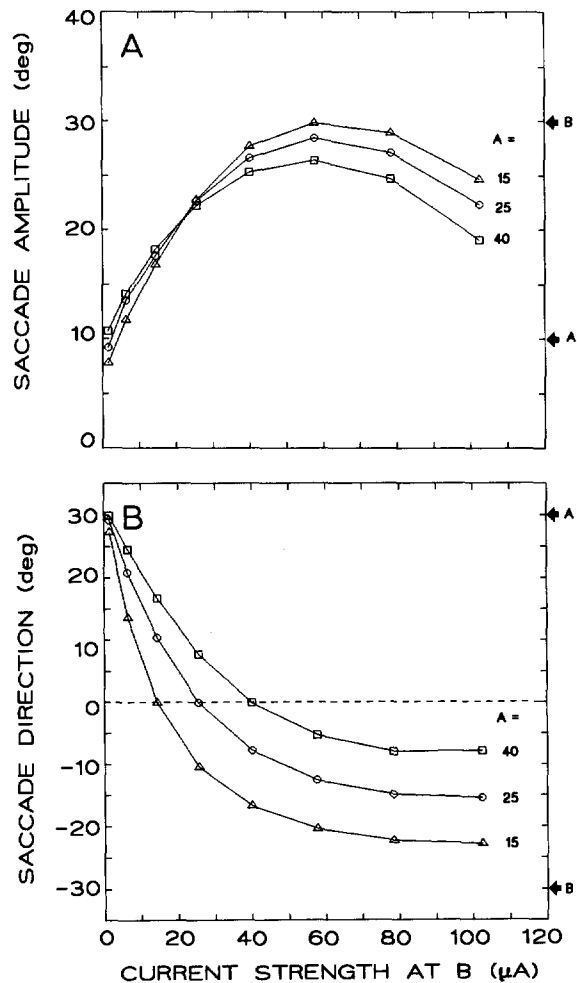


Fig. 8A and B. Summary of electrical double stimulation simulation results. In both boxes arrows marked A and B on the right-hand side denote the effect created by each stimulus in isolation. **A** ΔR -experiments. Saccade amplitude is plotted as a function of current strength at location u_B under three conditions: current strength at location u_A is $15 \mu\text{A}$ (triangles), $25 \mu\text{A}$ (circles) and $40 \mu\text{A}$ (rectangles), respectively. **B** $\Delta\Phi$ -experiment under the same conditions as in A. In all cases the saccade endpoint resembles a weighted average of the individual stimulation effects, A and B , with weighting factors reflecting the relative intensities of the two stimuli

tends to increase slightly under the 15 μA and 25 μA conditions. Saccade direction more and more approaches the direction of stimulus B as the intensity of stimulus B increases. In all cases examined, the saccade metrics resemble a weighted average of the individual stimulation effects, with weighting factors determined by the relative current strengths of the two stimuli. These findings are in qualitative agreement with Robinson's (1972) data (see Discussion).

5 Discussion

5.1 General Remarks

In this paper we have extended the linear ensemble coding model of Van Gisbergen et al. (1987) in order to explain two nonlinear phenomena which are known from electrical stimulation experiments in the deeper layers of the superior colliculus: 1) the finding that saccade amplitude is related to stimulus intensity above a certain threshold current, and 2) the fact that, in electrical double stimulation, the resulting saccade resembles the weighted average of the individual stimulation effects. We have shown in this paper that both phenomena may be the result of lateral inhibitory interactions among collicular movement cells. In the model the relative inhibition strength exerted by each cell on its neighbours is rather small ($B=0.0032\text{ mm}^{-2}$), but can still produce a significant effect by the combined action of many neurons. In the Introduction we have mentioned data from the literature which seem to justify the assumption of an intracollicular inhibitory mechanism. We will now discuss the results of our modified model more extensively.

5.2 The Amplitude vs. Current Strength Relation

The finding that beyond a certain current strength saccade amplitude does not increase further has often been noted (Robinson 1972; Schiller and Stryker 1972; Sparks and Mays 1983; see Schiller 1984; Sparks 1986, for extensive reviews). From data of Sparks and Mays (1983), however, it is known that for *low* stimulation intensities there is a relation between saccade amplitude and current strength. The general picture that emerges from ongoing experiments performed in our laboratory (to be published separately), is that saccade amplitude follows a roughly sigmoid function in the low current strength range ($<10\text{ }\mu\text{A}$). Quite remarkably, saccade *direction* shows hardly any change under these conditions. All of these findings can be simulated by the new model (Fig. 5).

It should be mentioned that if the saccadic system would compute the "center of gravity" of the stimulus configuration (Findlay 1982), one would not expect

any relation at all between saccade size and stimulus intensity (see above). Instead, the system appears to behave more or less linearly at low intensities and shows saturation at higher current strengths (see also below: extracollicular mechanisms).

We found that the precise nature of the saccade amplitude-current intensity relation in the model depends upon the shape of the lateral transmission function (2). In this paper we have explored the possibilities of a very simple (one free parameter) formulation for this function where the inhibition is supposed to be of constant strength throughout both colliculi. The curve, presented in Fig. 5, agrees only qualitatively with the Sparks and Mays (1983) data. The simulations give rise to two discrepancies that cannot be resolved with such a simple model:

First, the amplitude of the evoked saccade *overshoots* the saccade associated with maximum recruitment of nearby movement cells (the optimum or "best" saccade) by about 10% for the higher ($>40\text{ }\mu\text{A}$) current strengths (Fig. 5). There are no reports in the literature, to our knowledge, to support these findings.

Second, for extreme stimulus intensities ($>100\text{ }\mu\text{A}$) saccade amplitude decreases again (Fig. 5). This is probably an unrealistic finding. We have observed that when the inhibition profile [B in (2)] is taken to be Gaussian, the model's behaviour improves considerably in this respect. Lateral inhibition profiles with more parameters can probably solve both problems, at least in principle. One should bear in mind, however, that in contrast to the contiguous nature of the visual input and the motor output of the saccadic system, the internal representation in the colliculi is highly discontinuous: the right and left halves of motor space are represented in separate colliculi. Since, in the model, we have assumed that the lateral transmission function extends to *both* colliculi, a heuristic procedure would be needed to extend a non-constant profile to the other colliculus. Additional assumptions have to be made in such a case. In this paper we have not explored this point further.

5.3 Electrical Double Stimulation

The model, in its present form, can qualitatively explain the nonlinear interaction that is observed (Robinson 1972) when two electrical stimuli are applied simultaneously. A similar phenomenon is known to occur when both stimulating electrodes are situated in the frontal eye fields (Robinson and Fuchs 1969) or when frontal eye fields and colliculus are both electrically stimulated (Schiller and Sandell 1983). Also when the saccadic system is confronted with two visual stimuli, either presented simultaneously (Findlay 1982; Ottes et al. 1984), or sequentially as a double target-

step (Becker and Jürgens 1979) averaging responses can again be observed. In order to establish whether the observed behavioural effects are possibly due to the intracollicular mechanism described in this paper, pertinent electrophysiological experiments need to be performed.

An interesting implication from the simulations is the uncoupling of saccade metrics and population activity profile which generates the saccade (see e.g. Figs. 6 and 7). Despite the fact that the metrics of the resulting saccade can be identical for the $\Delta\Phi$ - as well as the ΔR -experiment, the activity profiles yielding that saccade are clearly different. Thus the new model can generate a given saccade through a variety of activation patterns in the motor map. Furthermore, the resulting saccade is not necessarily directed to the location which corresponds to maximal activity in the colliculus. This seems to contradict the notion that the colliculus encodes the metrical properties of a saccade through a tight relation with the locus of the activity profile (Sparks et al. 1976; McIlwain 1982). According to the new model, this picture would only be valid for saccades caused by a single stimulus.

Sparks and Mays' (1983) data showing that the electrical stimulation threshold for evoking a saccade increases significantly when the monkey is actively fixating a visual stimulus might be explained by the model if one assumes that in this case the activity in the foveal area exerts its inhibitory influence in both colliculi. More current will be needed to overcome this inhibition. For a similar explanation of a comparable phenomenon in frontal eye fields stimulation experiments, see Goldberg et al. (1986). If this idea is correct, study of fixation-induced threshold increases at various collicular stimulation sites could provide a quantitative estimate for the extent and the strength of the lateral inhibition.

5.4 Extracollicular Mechanism

This paper investigates the possibility of an intracollicular mechanism as an explanation for observed nonlinearities in saccade generation. It is assumed that the firing rate of individual movement cells in the deeper layers of the superior colliculus depends on the activity of all other cells. Instead, one can conceive of a model which scales the *efferent* output of a neuron dependent upon the total activity profile of the motor colliculus. Such a scheme explains the nonlinearities with an extracollicular mechanism. Suppose, that in this case (4) can be reformulated as:

$$\mathbf{M}_i(u, v) = \gamma \cdot F_i(u, v) \cdot \mathbf{P}_i(u, v),$$

where

$$\gamma = 1 / \left[\lambda + \sum_{i=1}^N F_i(u, v) \right]. \quad (5)$$

In (5) λ is a constant (spikes/s). In contrast to (4), where the proportionality constant is fixed (see above), γ now depends on the total activity in the colliculus. Assuming that for small values of N (corresponding to low stimulation intensities) λ dominates the numerator, (5) reduces to (4) and the system is linear. For high stimulus intensities λ may be neglected compared to the total number of spikes. In that case (5) approximates the "center of gravity" of the activity profile. Also in this model, saccade amplitude will depend in a sigmoid fashion on current intensity (see also Van Opstal and Van Gisbergen 1989). Reichardt et al. (1983) and Egelhaaf (1985) have put forward a model of the fly's visual system based on the notion of shunting inhibition. The overall transfer function of the output neurons in their model has the same characteristic as (5) (Reichardt et al. 1983). In such a scheme parameter λ is a measure for the strength of the shunting inhibition. At the moment, however, it is not clear how such a scheme can be applied to the monkey saccadic system.

In conclusion, we have shown how lateral inhibitory interactions in the deeper layers of the motor colliculus may explain the nonlinear behaviour of saccade metrics in electrical stimulation experiments. Further neurophysiological and theoretical work will be needed to get a better insight in the neural wiring diagram that may underly these interactions.

Acknowledgements. The authors are indebted to Gerard Hesselmans, Peter Penders, Peter Johannesma and Stan Gielen for computational assistance and valuable discussions. This study was supported by the Netherlands Organization for the Advancement of Pure Research (NWO) and the BRAIN research program of the EC.

6 Appendix

1 Relation Between Current Strength And Excitatory Profile

It has been shown in the literature (e.g. Stoney et al. 1968; Alexander and Delong 1985) that the minimal current, I [μA], needed to excite a neuron at distance r [mm] from the electrode tip is given by:

$$I = k + m \cdot r^2, \quad (A1)$$

where k [μA] is the minimal threshold current needed to excite the cell when the electrode is at its soma and m [$\mu\text{A}/\text{mm}^2$] is a proportionality constant. Both parameters are physiological constants which not only reflect physical conduction properties of the physiological medium but also characteristics of the neural network under study.

Since quantitative parameter estimates for k and m are not available for the monkey colliculus it was not possible to base the dimensions of the excitation zone

for each current strength on literature data. Assuming that (5) remains qualitatively valid also in this case, the afferent excitation width, σ_a , is directly related to current strength through (5) (see e.g. Stoney et al. 1968, their Fig. 7). Taking $r=2 \cdot \sigma_a$ as the boundary of effective excitation, it is easy to show that

$$\sigma_a = 0.5 \cdot [(I-k)/m]^{1/2}. \quad (A2)$$

In our model we assume that increasing the strength of the stimulation current leads to an increase of the spatial spread, σ_a , of the excitation zone in (1) without changing the maximal excitatory effect, E_{\max} . Furthermore, instead of relating the intensity of the electrical stimulus to the all-or-nothing firing of a given neuron (Stoney et al. 1968), it is assumed that the applied current gives rise to a depolarization (expressed in mV) of the cell's membrane (1). Since it is a consistent finding that the current threshold for the deeper layers of the monkey colliculus, needed to elicit a saccadic eye movement, is very low (usually between 1–9 μA ; Schiller and Stryker 1972), we have set the k value at 0 μA . This is the reason why in Fig. 5 saccade amplitude is 0 deg for $I=0$ but increases immediately when current is applied. In a more realistic situation one should also incorporate k -values which are not equal to zero. Figure 4 depicts how spatial extent, σ_a , and current intensity, I , are related in our model for $k=0 \mu\text{A}$ and $m=40 \mu\text{A}/\text{mm}^2$. These parameters were chosen so as to produce a spatial spread of $\sigma_a=0.5 \text{ mm}$ at a current intensity of 40 μA (Stoney et al. 1968 their Fig. 7 and McIlwain 1982).

II Population Profile Width as a Function of σ_a

As can be seen in Fig. 5, the model predicts that saccade amplitude increases with current strength for low stimulus intensities, reaches a maximum level in the range between 40–90 μA , but finally starts to decrease for high current strengths. To explore why the model yields this result we will now analyse mathematically the width of the excited population as a function of current strength. It is straightforward to show that the membrane potential, $C(u, v)$, of a movement cell at (u, v) can be derived from (3) as:

$$C(u, v) = E_{\max} \cdot T_{\max} \cdot \exp \left[-\frac{(u-u_c)^2 + (v-v_c)^2}{2\sigma_a^2} \right] - 2 \cdot \pi \cdot E_{\max} \cdot B \cdot \sigma_a^2. \quad (A3)$$

Note, that (A3) describes indeed a Gaussian excitatory profile, surrounded by constant inhibition (see Fig. 3C). The negative inhibition term is related to σ_a and hence depends on current strength (Fig. 4 and (A2)).

The dimensions of the proportionality constants can now be established. Since $C(u, v)$ is expressed in

milliVolts, the two quantities $E_{\max} \cdot T_{\max}$ and $B \cdot E_{\max} \cdot \sigma_a^2$ also must yield a voltage. It follows that if $E_{\max} = [\text{mV}]$, $T_{\max} = \text{dimensionless}$ and $B = [\text{mm}^{-2}]$.

In order to understand the behaviour of saccade amplitude in the new model, we need to determine the boundary of excitation [i.e. $C(u, v)=0$], since it is assumed that only cells that are excited contribute to the saccade (4). Setting (A3) to 0 yields:

$$\varrho(\sigma_a) = \sigma_a \cdot \left[\ln \left(\frac{T_{\max}^2}{2 \cdot \pi \cdot B^2 \cdot \sigma_a^2} \right) \right]^{1/2} \quad (A4)$$

for the radius ϱ of the population activity profile. Note that ϱ is determined by the relative inhibition strength, T_{\max}/B , and excitation width, σ_a , but is independent of E_{\max} . It can easily be shown that ϱ reaches a maximum value (which is the maximum population width) and decreases for higher σ_a values. The behaviour of (A4) underlies the properties of saccade amplitude as a function of current strength (Fig. 5).

References

- Alexander GE, Delong HR (1985) Microstimulation of the primate neostriatum. I. Physiological properties of striatal microexcitable zones. *J Neurophysiol* 53:1401–1416
- Becker W, Jürgens R (1979) An analysis of the saccadic system by means of double step stimuli. *Vision Res* 19:967–983
- Carpenter RHS (1977) *Movements of the eyes*. Pion, London
- Douglas RM, Vetter M (1986) Widespread inhibition and target selection in the superior colliculus. *Soc Neurosci (abstr)* 12:458
- Egelhaaf M (1985) On the neuronal basis of figure-ground discrimination by relative motion in the visual system of the fly. I. Behavioural constraints imposed on the neuronal network and the role of the optomotor system. *Biol Cybern* 52:123–140
- Ferman L, Collewijn H, Van den Berg AV (1987) A direct test of Listing's law. II. Human ocular torsion measured under dynamic conditions. *Vision Res* 27:939–951
- Findlay JM (1982) Global visual processing for saccadic eye movements. *Vision Res* 22:1033–1045
- Goldberg ME, Bushnell MC, Bruce CJ (1986) The effect of attentive fixation on eye movements evoked by electrical stimulation of the frontal eye fields. *Exp Brain Res* 61:579–584
- Infante C, Leiva J (1986) Simultaneous unitary neuronal activity in both superior colliculi and its relation to eye movements in the cat. *Brain Res* 381:390–392
- McIlwain JT (1976) Large receptive fields and spatial transformations in the visual system. *Int Rev Physiol* 10:223–248
- McIlwain JT (1982) Lateral spread of neural excitation during microstimulation in intermediate gray layer of cat's superior colliculus. *J Neurophysiol* 47:167–178
- Ottes FP, Van Gisbergen JAM, Eggermont JJ (1984) Metrics of saccade responses to visual double stimuli: two different modes. *Vision Res* 24:1169–1179
- Ottes FP, Van Gisbergen JAM, Eggermont JJ (1986) Visuomotor fields of the superior colliculus: a quantitative model. *Vision Res* 26:857–873

- Reichardt W, Poggio T, Hausen K (1983) Figure-ground discrimination by relative movement in the visual system of the fly. Part II. Towards a neural circuitry. *Biol Cybern* 46 [Suppl]:1-30
- Rizzolatti G, Camarda R, Grupp LA, Pisa M (1973) Inhibition of visual responses of single units in the cat superior colliculus by the introduction of a second visual stimulus. *Brain Res* 61:390-394
- Rizzolatti G, Camarda P, Grupp LA, Pisa M (1974) Inhibitory effect of remote visual stimuli on visual response of cat superior colliculus: spatial and temporal factors. *J Neurophysiol* 37:1262-1275
- Robinson DA (1972) Eye movements evoked by collicular stimulation in the alert monkey. *Vision Res* 12:1795-1807
- Robinson DA, Fuchs AF (1969) Eye movements evoked by stimulation of frontal eye fields. *J Neurophysiol* 32:637-648
- Schiller PH (1984) The superior colliculus and visual function. In: Brookhart JM, Mountcastle VB (eds) *Handbook of physiology*, vol III. American Physiological Society, Md, USA
- Schiller PH, Sandell JH (1983) Interactions between visually and electrically elicited saccades before and after superior colliculus ablations in the rhesus monkey. *Exp Brain Res* 49:381-392
- Schiller PH, Stryker M (1972) Single-unit recording and stimulation in superior colliculus of the alert rhesus monkey. *J Neurophysiol* 35:915-924
- Schiller PH, Sandell JH, Maunsell JHR (1987) The effect of frontal eye field and superior colliculus lesions on saccadic latencies in the rhesus monkey. *J Neurophysiol* 57:1033-1049
- Sparks DL (1986) Translation of sensory signals into commands for control of saccadic eye movements: role of primate superior colliculus. *Physiol Rev* 66:118-171
- Sparks DL, Mays LE (1980) Movement fields of saccade-related burst neurons in the monkey superior colliculus. *Brain Res* 190:39-50
- Sparks DL, Mays LE (1983) Spatial localization of saccade targets. I. Compensation for stimulation-induced perturbations in eye position. *J Neurophysiol* 49:45-63
- Sparks DL, Holland R, Guthrie BL (1976) Size and distribution of movement fields in the monkey superior colliculus. *Brain Res* 113:21-34
- Stoney SD Jr, Thompson WD, Asanuma H (1968) Excitation of pyramidal tract cells by intracortical microstimulation: effective extent of stimulating current. *J Neurophysiol* 31:659-669
- Van Gisbergen JAM, Van Opstal AJ, Tax AAM (1987) Collicular ensemble coding of saccades based on vector summation. *Neuroscience* 21:541-555
- Van Opstal AJ, Van Gisbergen JAM (1987) A nonlinear model of collicular spatial interactions possibly underlying saccadic averaging responses to electrical double stimulation. *Neuroscience* 22 [Suppl]:847
- Van Opstal AJ, Van Gisbergen JAM (1989) A model for collicular efferent mechanisms underlying the generation of saccades. *Brain Behav Evol* (in press)
- Wurtz RH, Goldberg ME (1972) Activity of superior colliculus in behaving monkey. III. Cells discharging before eye movements. *J Neurophysiol* 35:575-586
- Wurtz RH, Richmond BJ, Judge SJ (1980) Vision during saccadic eye movements. III. Visual interactions in monkey superior colliculus. *J Neurophysiol* 43:1168-1181

Received: March 3, 1988

Dr. A. J. Van Opstal
 Department of Medical Physics and Biophysics
 University of Nijmegen
 Geert Grooteplein Noord 21
 6526 EZ Nijmegen
 The Netherlands